Role of the N- and C-Terminal Domains in Binding of Apolipoprotein E Isoforms to Heparan Sulfate and Dermatan Sulfate: A Surface Plasmon Resonance Study[†]

Yuko Yamauchi,[‡] Noriko Deguchi,[‡] Chika Takagi,[§] Masafumi Tanaka,[§] Padmaja Dhanasekaran,[||] Minoru Nakano,[‡] Tetsurou Handa,[‡] Michael C. Phillips,[||] Sissel Lund-Katz,*[,||] and Hiroyuki Saito[§]

Graduate School of Pharmaceutical Sciences, Kyoto University, Kyoto 606-8501, Japan, Department of Biophysical Chemistry, Kobe Pharmaceutical University, Kobe 658-8558, Japan, and Lipid Research Group, The Children's Hospital of Philadelphia, University of Pennsylvania School of Medicine, Philadelphia, Pennsylvania 19104-4318

Received March 7, 2008; Revised Manuscript Received May 2, 2008

ABSTRACT: The ability of apolipoprotein E (apoE) to bind to cell-surface glycosaminoglycans (GAGs) is important for lipoprotein remnant catabolism. Using surface plasmon resonance, we previously showed that the binding of apoE to heparin is a two-step process; the initial binding involves fast electrostatic interaction, followed by a slower hydrophobic interaction. Here we examined the contributions of the N- and C-terminal domains to each step of the binding of apoE isoforms to heparan sulfate (HS) and dermatan sulfate (DS). ApoE3 bound to less sulfated HS and DS with a decreased favorable free energy of binding in the first step compared to heparin, indicating that the degree of sulfation has a major effect on the electrostatic interaction of GAGs with apoE. Mutation of a key Lys residue in the N-terminal heparin binding site of apoE significantly affected this electrostatic interaction. Progressive truncation of the C-terminal α-helical regions which favors the monomeric form of apoE3 greatly weakened the ability of apoE3 to bind to HS, with a much reduced favorable free energy of binding of the first step, suggesting that the C-terminal domain contributes to the GAG binding of apoE by the oligomerization effect. In agreement with this, dimerization of the apoE3 N-terminal fragment via disulfide linkage restored the electrostatic interaction of apoE with HS. Significantly, apoE4 exhibited much stronger binding to HS and DS than apoE2 or apoE3 in both lipid-free and lipidated states, perhaps resulting from enhanced electrostatic interaction through the N-terminal domain. This isoform difference in GAG binding of apoE may be physiologically significant such as in the retention of apoE-containing lipoproteins in the arterial wall.

Heparan sulfate proteoglycan (HSPG)[1] is a common constituent of cell surfaces and the extracellular matrix and is involved in a wide range of biological functions (*1*). Normal uptake and catabolism of atherogenic lipoproteins are mediated by the interaction of lipoproteins with heparan sulfate (HS) in the liver (*2*). The substantial reduction of the level of hepatic HS sulfation associated with diabetes (*3*) is known to cause impaired hepatic uptake of lipoproteins, leading to increased levels of atherosclerosis (*4*). Apolipoprotein E (apoE) is a critical ligand for high-affinity binding of remnant lipoproteins to members of the low-density lipoprotein receptor (LDLR) family and HSPG (*5–7*). Binding of apoE to HSPG is an initial step in the localization of apoE-enriched remnant lipoproteins to the cell surface, followed by the internalization into hepatocytes through processes mediated by receptors, including the LDLR and the LDLR-related protein, or through interaction with HSPG alone (*8*). Binding of apoE to HSPG is also involved in the inhibition of platelet-derived growth factor-stimulated smooth muscle cell proliferation (*9*) and the differential effects of the apoE isoforms on neurite growth, repair, and, consequently, the progression of late onset familiar Alzheimer's disease (*10–12*).

Besides the apoE−HSPG interaction, the binding of apoE to cell-surface glycosaminoglycans (GAGs) such as chondroitin sulfate (CS) and dermatan sulfate (DS) proteoglycans has been demonstrated to play an important role in lipoprotein catabolism. A major pool of apoE on the surface of human liver cells is associated with CS proteoglycans (*13*). The interaction of apoE with CS and/or DS proteoglycans is responsible for the retention of high-density lipoproteins (HDLs) on the extracellular matrix of arterial smooth muscle cells (*14*), and the uptake of β-very low density lipoprotein in the brain (*15*). In addition, apoE-mediated cholesterol efflux from macrophages is modulated by cell-surface proteoglycans (*16, 17*).

[†] This work was supported by NIH Grant HL56083, Grants-in-Aid for Scientific Research from JSPS (Grants 17390011 and 19590048), the Naito Foundation, and the NOVARTIS Foundation (Japan) for the Promotion of Science.

* To whom correspondence should be addressed: The Children's Hospital of Philadelphia, Abramson Research Center, Suite 1102, 3615 Civic Center Blvd., Philadelphia, PA 19104-4318. Telephone: (215) 590-0588. Fax: (215) 590-0583. E-mail: katzs@email.chop.edu.

[‡] Kyoto University.

[§] Kobe Pharmaceutical University.

[||] University of Pennsylvania School of Medicine.

[1] Abbreviations: apoE, apolipoprotein E; CD, circular dichroism; CS, chondroitin sulfate; DMPC, dimyristoylphosphatidylcholine; DS, dermatan sulfate; GAG, glycosaminoglycan; GdnHCl, guanidine hydrochloride; HS, heparan sulfate; HSPG, heparan sulfate proteoglycan; HDL, high-density lipoprotein; LDLR, low-density lipoprotein receptor; SPR, surface plasmon resonance; RU, resonance unit; WT, wild type.

10.1021/bi8003999 CCC: $40.75
Published on Web 05/29/2008

ApoE contains two independently folded functional domains; these are a 22 kDa N-terminal domain (residues 1−191) and a 10 kDa C-terminal domain (residues 216−299) linked by a hinge region (*18, 19*). The N-terminal domain is folded into a four-helix bundle of amphipathic α-helices and contains the LDLR binding region (around residues 136−150 in helix 4) (*20*), whereas the C-terminal domain contains amphipathic α-helices that are involved in binding to lipoproteins with high affinity (*21, 22*). Both the N- and C-terminal domains contain a heparin binding site (*23, 24*): the N-terminal domain site is located between residues 136 and 147, overlapping with the LDLR binding region (*25, 26*), whereas the C-terminal site involves basic residues around lysine 233 (*27*). Although both sites are functional in the separated fragments, only the N-terminal site is available for interaction in both the lipid-free and lipidated states of the intact apoE molecule (*27, 28*). The C-terminal site may be involved in the binding of apoE to the protein core of biglycan of the vascular extracellular matrix (*29, 30*).

Given the physiological importance of apoE−GAG interactions, we have previously characterized the kinetics and affinity of the binding of apoE isoforms to heparin using surface plasmon resonance (SPR) measurements (*28*). Although the variations in the distribution of acidic groups in different types of GAGs (*31*) are likely to influence the interaction with apoE (*32, 33*), quantitative information about the interaction with various GAG molecules is limited (*26, 34*). In this study, we extended the SPR approach to explore the contributions of the N- and C-terminal domains of apoE to its interaction with more physiological GAGs, such as HS and DS.

EXPERIMENTAL PROCEDURES

Materials. Porcine intestinal mucosa HS (average molecular weight of 13655, sulfur content of 5.51%), DS (average molecular weight of 41400, sulfur content of 6.85%), and heparin (average molecular weight of 13000, sulfur content of <38%) were purchased from Celsus Laboratories (Cincinnati, OH). Degrees of sulfation determined by the turbidimetry method (*35*) were 1.6, 0.7, and 0.7 sulfate groups per disaccharide for heparin, HS, and DS, respectively. 1,2-Dimyristoylphosphatidylcholine (DMPC) was purchased from Avanti Polar Lipids (Pelham, AL), and stock solutions were stored in a chloroform/methanol mixture (2/1) under nitrogen at −20 °C. Ultrapure guanidine HCl was from ICN Pharmaceuticals (Costa Mesa, CA).

Protein Preparations. Full-length human apoE2, apoE3, and apoE4 and their 22 kDa (residues 1−191) fragments were expressed and purified as described previously (*22, 36*). The mutations in apoE to create K146E and K233E, and the truncated forms (Δ251−299, Δ261−299, and Δ273−299) were made using PCR methods as described previously (*27, 37*). The apoE preparations were at least 95% pure as assessed by SDS−PAGE. In all experiments, the apoE sample was freshly dialyzed from a 6 M GdnHCl and 1% β-mercaptoethanol (or 10 mM DTT) solution into a buffer solution before use. To prepare the dimerized form of apoE3 22 kDa, the apoE3 22 kDa fragment at 10 mg/mL in oxygenated Tris buffer [10 mM Tris-HCl, 150 mM NaCl, 0.02% NaN_3, and 1 mM EDTA (pH 7.4)] in the presence 6 M urea was incubated for 2 weeks at 4 °C. Residual monomer was removed by passing the sample through a Thiopropyl Sepharose 6B column (GE Healthcare). DMPC discoidal complexes with the apoE3 variants were prepared as described previously (*38*).

Biotinylation of GAGs. Heparin, HS, and DS were biotinylated at their reducing end (*39, 40*). Heparin, HS, or DS (4.5 mg/mL) was oxidized with 3.3 mM sodium metaperiodate (Wako Pure Chemicals, Osaka, Japan) in 0.1 M sodium acetate (pH 5.5) for 1 h at room temperature. The oxidation was stopped by adding an excess of sodium sulfite. The oxidized GAG was then incubated with a 6-fold molar excess of 6-(biotinylamino)hexanoylhydrazine (Dojindo Laboratories, Kumamoto, Japan) for 2 h. The excess biotin was removed by dialysis.

SPR Experiments. SPR measurements were performed on a Biacore X instrument (Biacore, Inc., Uppsala, Sweden) (*28*). For immobilization of GAG on a SA chip, an injection of biotinylated GAG (10 μg/mL) in Tris buffer was made at a flow rate of 5 μL/min followed by a 10 μL injection of 2 M NaCl. Typically, 100−500 resonance units (RU) of GAG was immobilized, and the effects of mass transport were not significant due to the low surface density of the ligand (*41*). An untreated flow cell was used as a control. For kinetic measurement of the interaction of apoE with GAG, a 30 μL injection of the apoE sample was passed over the sensor surface at a flow rate of 20 μL/min. At the end of the sample plug, the same buffer was passed over the sensor surface to facilitate dissociation, and then the sensor surface was regenerated for the next sample using a 10 μL pulse of 2 M NaCl and 0.1% CHAPS. The resultant sensorgrams were analyzed using BIA evaluation (version 4.1). The response curves of various analyte concentrations were globally fitted to the two-state binding model described by the following equation (*42, 43*):

$$A + B \underset{k_{d1}}{\overset{k_{a1}}{\leftrightarrow}} AB \underset{k_{d2}}{\overset{k_{a2}}{\leftrightarrow}} AB_x \quad (1)$$

where the equilibrium constants of the each binding steps are K_1 (k_{a1}/k_{d1}) and K_2 (k_{a2}/k_{d2}) and the overall equilibrium binding constant is calculated as $K_A = K_1(1 + K_2)$ and $K_d = 1/K_A$. In this model, the analyte (A) binds to the ligand (B) to form an initial complex (AB) and then undergoes subsequent binding or conformational change to form a more stable complex (AB_x). Gibbs free energies of binding of each binding step are calculated according to the relationships $\Delta G_1 = -RT \ln(55.5K_1)$ and $\Delta G_2 = -RT \ln K_2$, respectively. The maximum binding response (R_{max}) value which reflects the saturated amount of apoE bound to GAG was obtained from the global fitting.

Circular Dichroism (CD) Spectroscopy. Far-UV CD spectra were recorded from 185 to 260 nm at 25 °C using an Aviv 62DS spectropolarimeter. After dialysis, the apoE sample was diluted to 25−50 μg/mL in 10 mM phosphate buffer (pH 7.4) to yield the CD spectrum. The results were corrected by subtracting the buffer baseline. The α-helix content was derived from the molar ellipticity at 222 nm, $[\theta]_{222}$, according to the following equation (*44*):

$$\%\ \alpha\text{-helix} = (-[\theta]_{222} + 3000)/(36000 + 3000) \times 100 \quad (2)$$

Fluorescence Measurements. Fluorescence measurements were carried out with a Hitachi F-7000 fluorescence spectrophotometer at 25 °C in Tris buffer (pH 7.4). Trp emission

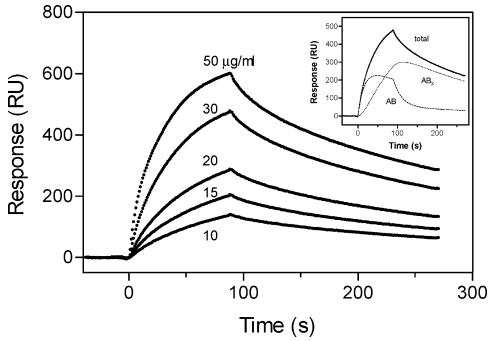

FIGURE 1: SPR sensorgrams of binding of lipid-free apoE3 to immobilized HS. The inset shows the fitting of experimental data (●) with the two-state binding model, where A + B ↔ AB ↔ AB$_x$ (see Experimental Procedures). Simulated curves displaying the initial binding (AB) and subsequent binding (AB$_x$) are the additive components from the fitted curve (—).

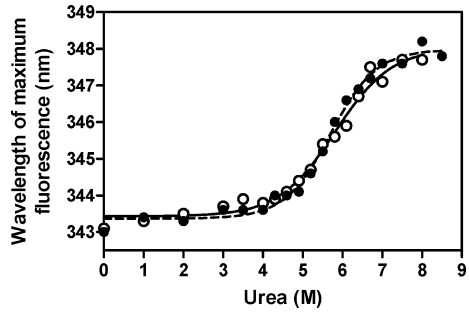

FIGURE 2: Urea denaturation of the apoE3 22 kDa fragment in the absence or presence of HS. The protein concentration was 25 μg/mL. ApoE3 22 kDa fragment alone (○) or incubated with 50 μg/mL HS (●).

fluorescence of proteins at a concentration of 25 μg/mL was recorded from 300 to 420 nm using a 295 nm excitation wavelength to prevent tyrosine fluorescence. For chemical denaturation experiments, the change in the wavelength of maximum fluorescence was monitored at various urea concentrations in the absence or presence of HS.

Statistical Analysis. Results were compared statistically with a *t* test using GraphPad Prism 5.0.

RESULTS

Two-Step Binding of ApoE to GAG. We previously demonstrated that the binding of apoE to heparin is a two-step process; the initial binding involves fast electrostatic interaction, followed by a slower hydrophobic interaction (*28*). Figure 1 shows typical sensorgrams for the binding of lipid-free apoE3 to HS. The response curves were fitted well by a two-state binding model in which binding of the analyte to the ligand is followed by either another subsequent binding event or a conformational change (Figure 1, inset). In far-UV CD measurements, no change in the spectra of apoE3 was observed in the absence or presence of HS (data not shown). In addition, HS had no effect on the urea-induced denaturation behavior of the apoE3 22 kDa fragment (Figure 2). These results suggest that there is no major conformational change in apoE upon HS binding. Similar two-step binding was also observed in the binding of lipid-free apoE3 to DS (data not shown).

Figure 3 summarizes the relative changes in the rate constants for each step of lipid-free apoE3 binding to GAG (Figure 3A) and the relative contributions of each step to

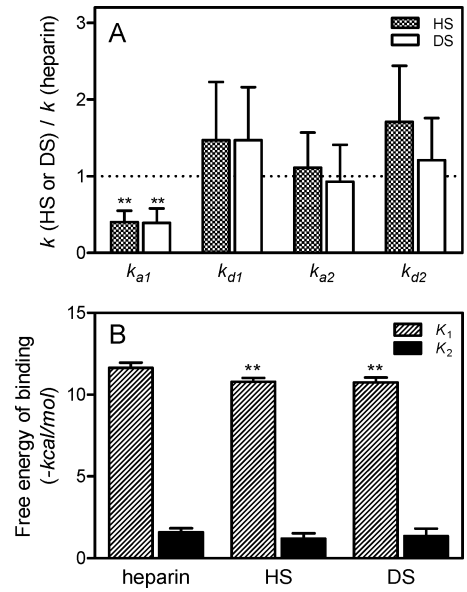

FIGURE 3: SPR rate constants and free energy of binding for the interaction of lipid-free apoE3 with GAG. (A) Relative change in SPR rate constants for each step of binding of apoE3 to GAG. (B) Free energy for each step of binding of apoE3 to GAG. The free energy was calculated according to the relationship $\Delta G = -RT \ln K$ using binding constants for each steps, K_1 and K_2. Asterisks indicate a p of <0.01 vs heparin.

the overall free energy of binding estimated from the affinity constants for the two individual steps (Figure 3B). Compared to heparin, the less sulfated HS and DS exhibited a slower first association rate and, consequently, a significant decrease in the favorable free energy of binding for the first step. This indicates that the degree of sulfation in GAG has a major effect on the electrostatic interaction with apoE (*26*).

Effects of Lysine Mutations in the Heparin Binding Sites of ApoE on GAG Binding. To confirm the importance of an ionic interaction in the apoE−GAG interaction, we examined the effects of substitutions of lysine residues 146 and 233 in apoE on GAG binding; these residues are located in the N- and C-terminal heparin binding sites, respectively, and contribute to an ionic interaction with heparin (*26, 27*). As shown in Figure 4A, large decreases in the extent of binding to HS and DS were observed with the K146E mutant, whereas the K233E mutant exhibited responses similar to that of the WT, consistent with the previous finding that only the N-terminal site is available for the interaction with heparin even in the lipid-free state (*27, 28*). Comparison of the free energy of binding for each step among lysine mutants (Figure 4B) clearly demonstrates that such decreases in the extent of GAG binding for the K146E mutant are due to the weakening of the electrostatic interaction between apoE and GAG (*28*). In addition, such a disruption of the electrostatic interaction resulted in a decrease in the saturated amount of apoE bound to GAG: for example, R_{max} values for the HS binding of apoE3 WT, K146E, and K233E were 1300, 180, and 1020 RU, respectively.

Effects of Oligomerization of ApoE on GAG binding. ApoE is known to self-associate through the C-terminal domain in solution, and the C-terminal α-helical regions are responsible for the self-association (*21, 45–47*). To examine the role of the self-association of apoE in GAG binding, we compared the HS binding of progressive C-terminally truncated mutants of apoE3. Using gel filtration chromatography, we showed

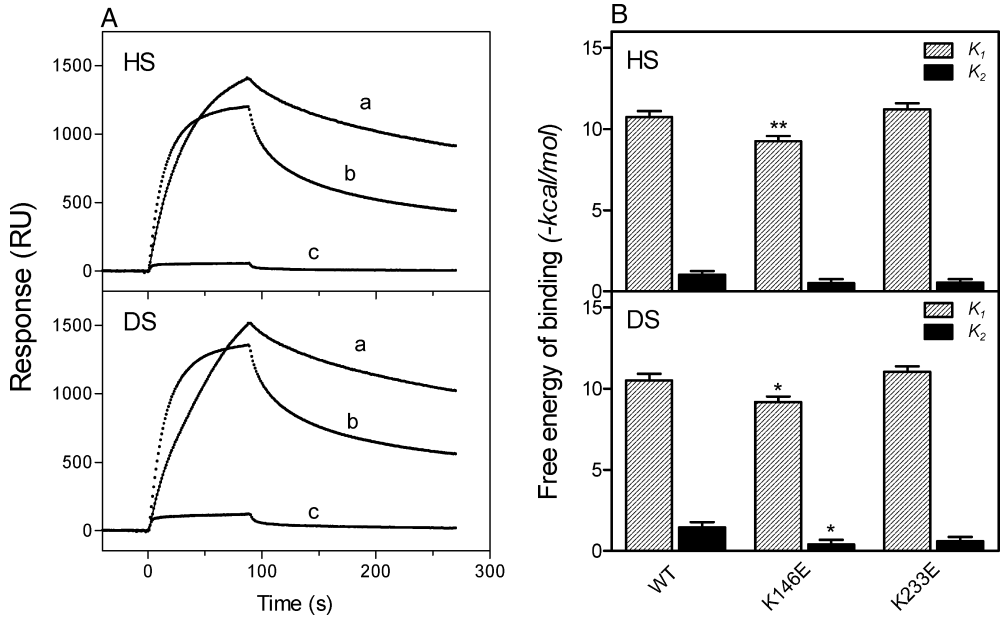

FIGURE 4: SPR sensorgrams (A) and free energies of binding (B) for the interaction of Lys mutants of apoE3 with HS and DS. (A) WT apoE3 (a), apoE3 K233E (b), and apoE3 K146E (c). The protein concentration was 30 μg/mL. (B) Free energy for each step of binding of apoE3 to HS and DS. One asterisk indicates a p of <0.05 vs WT, and two asterisks indicate a p of <0.01 vs WT.

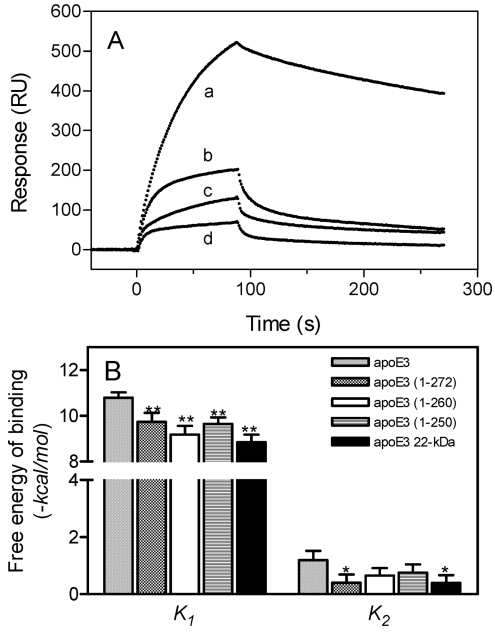

FIGURE 5: Effect of C-terminal truncation on the interaction of lipid-free apoE3 with HS. (A) SPR sensorgrams of binding of apoE3 C-terminally truncated mutants to HS: apoE3 (a), apoE3(1−272) (b), apoE3(1−260) (c), and apoE3 22 kDa fragment (d). The protein concentration was 30 μg/mL. (B) Free energies for each step of binding of apoE3 C-terminally truncated mutants.

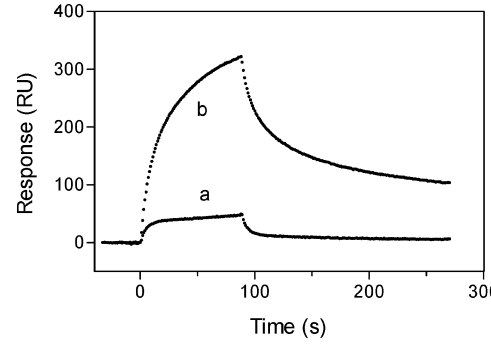

FIGURE 6: SPR sensorgrams of binding of apoE3 22 kDa variants to HS: apoE3 22 kDa monomer (a) and apoE3 22 kDa dimer (b). The protein concentration was 20 μg/mL.

previously that, even at a very low protein concentration (5 μg/mL), full-length apoE3 predominantly forms tetramer and that more than half of apoE3(1−272) forms tetramer whereas apoE3(1−260) exists completely as a monomer (*47*). Although the C-terminal heparin binding site is conserved in both apoE3(1−272) and apoE3(1−260), significant decreases in the binding response (Figure 5A) and favorable free energy of binding in the first step (Figure 5B) were observed for both mutants. This indicates that the oligomerization through the C-terminal α-helical regions has a major influence on the electrostatic interaction between apoE and GAG. However, R_{max} values were not significantly different among all mutants (880, 840, 1200, and 710 RU for full-length, 1−272, 1−260, and 1−250 apoE3, respectively), suggesting that the oligomerization does not affect the level of apoE binding to GAG.

It is possible that the better binding of oligomeric apoE compared to that of the monomeric form is due to cooperative molecular interaction of apoE with GAG. To confirm this point, we compared the binding behaviors of the apoE3 22 kDa fragment to HS in the monomeric and dimeric states. As shown in Figure 6, a greatly increased response in HS binding of the apoE3 22 kDa dimer was observed compared to the monomeric form, and the kinetic parameters for the apoE3 22 kDa dimer are comparable to those for full-length apoE3 (Table 1). In contrast, R_{max} values for the monomer and dimer were similar (1050 and 1250 RU, respectively). These results suggest that the cooperative binding through multiple copies of the heparin binding sites of apoE molecules is important for the high-affinity binding to GAG (*27*).

Effects of Lipidation on GAG Binding of ApoE. Although lipid-free apoE can bind effectively to GAG, we demonstrated previously that a discoidal complex of apoE 22 kDa fragments with DMPC exhibited much higher affinity in binding to heparin compared to the lipid-free form, mainly

Table 1: Kinetic Parameters for Binding of Lipid-Free ApoE3 Variants to HS

	k_{a1} ($\times 10^4$ M^{-1} s^{-1})	k_{d1} ($\times 10^{-2}$ s^{-1})	k_{a2} ($\times 10^{-2}$ s^{-1})	k_{d2} ($\times 10^{-3}$ s^{-1})	K_1 ($\times 10^5$ M^{-1})	K_2	K_d (μM)
apoE3	3.6 ± 0.6	2.5 ± 0.8	3.1 ± 1.0	4.2 ± 0.8	15	7.4	0.18 ± 0.03
apoE3 22 kDa	1.0 ± 0.6	20 ± 5	0.8 ± 0.3	4.2 ± 1.1	0.6	1.9	6.2 ± 2.9
apoE3 22 kDa dimer	2.7 ± 0.8	6.8 ± 1.8	1.4 ± 0.4	4.4 ± 0.5	4.1	3.1	0.61 ± 0.12

due to the increased free energy of binding in the first step (*28*). As shown in Figure 7A, similar effects of lipidation on the binding of the apoE3 22 kDa fragment to HS and DS were observed. In contrast, there was no significant increase but rather a tendency toward a decrease in the free energy of the first binding step between the lipid-free and lipidated forms of full-length apoE3 (Figure 7B), suggesting that the electrostatic interactions of full-length apoE with GAG are similar in the lipid-free and lipidated forms.

Effects of ApoE Isoforms on GAG Binding. We further compared the association and dissociation kinetics for the interaction of apoE isoforms with GAG. As shown in Figure 8, apoE4 displayed 2- or 3-fold greater binding to HS and DS compared to apoE2 or apoE3, respectively, in both the lipid-free and lipidated states. In fact, R_{max} values for lipid-free apoE2, apoE3, and apoE4 were 670, 810, and 1210, respectively, and those for the DMPC disks were 360, 320, and 635, respectively. Such stronger binding of apoE4 does not appear to result from the interaction between the N- and C-terminal domains in apoE4 because the apoE4 E255A mutant in which the domain interaction is disrupted (*48*) still exhibited much stronger binding than apoE3 (Figure 8A,B). As shown in Table 2, there was not much difference in association and dissociation rate constants and equilibrium affinity among apoE isoforms complexed with DMPC.

To explore why apoE4 binds better to GAG than other isoforms, the association and dissociation kinetics for the GAG binding of the 22 kDa fragments of apoE3 and apoE4 complexed with DMPC were compared. Although the binding level of apoE4 was similar to that of apoE3, apoE4 exhibited a faster first association, followed by a slower second step compared to apoE3 (Figure 9A). Consequently, the free energy of binding for the first step tended to increase and decrease for the second step for apoE4 compared to apoE3 (Figure 9B). This suggests that the increased extent of binding of full-length apoE4 to GAG comes from enhanced electrostatic interaction through the N-terminal binding site (*49*).

DISCUSSION

The various anti-atherogenic functions of apoE, such as facilitated remnant lipoprotein uptake by the liver (*8, 50*) and cholesterol efflux from macrophages (*16, 17*), are achieved through its interaction with cell-surface GAG. Because receptor−ligand interactions at the cell surface do not occur at equilibrium, it is important to establish the kinetics of apoE−GAG association and dissociation. On the basis of SPR measurements to characterize the kinetics and affinity of binding of apoE to heparin, we previously

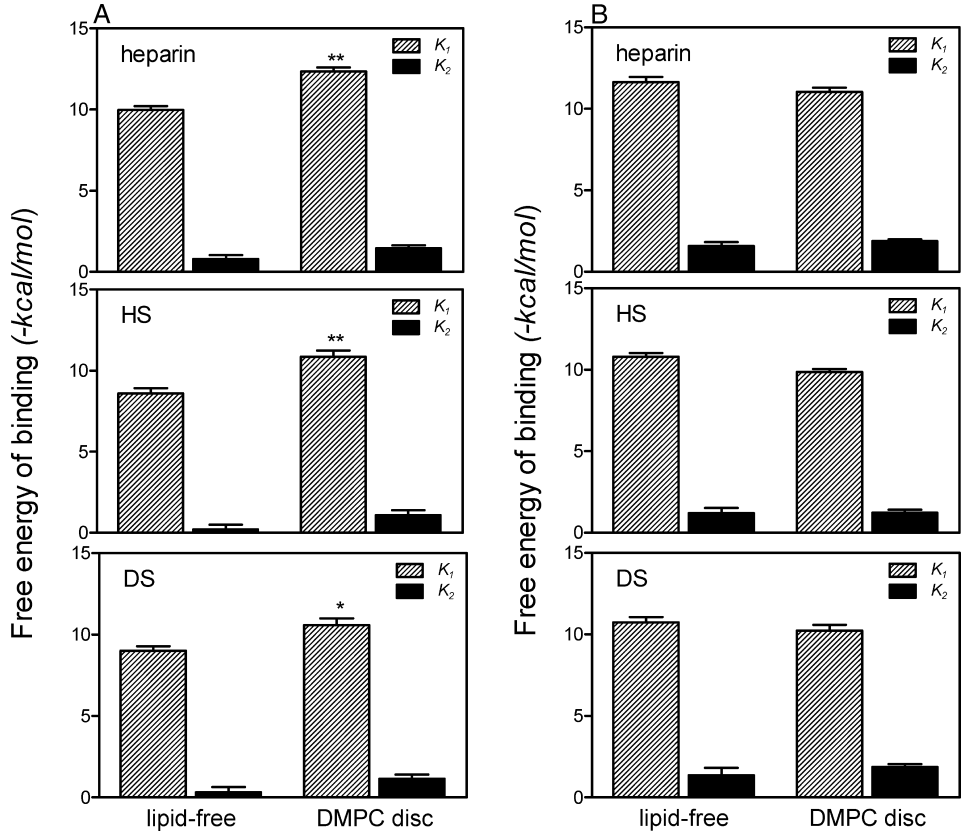

FIGURE 7: Comparison of free energies for GAG binding of apoE3 in the lipid-free form or complexed with DMPC: (A) apoE3 22 kDa and (B) full-length apoE3. One asterisk indicates a p of <0.05 vs the lipid-free form, and two asterisks indicate a p of <0.01 vs the lipid-free form.

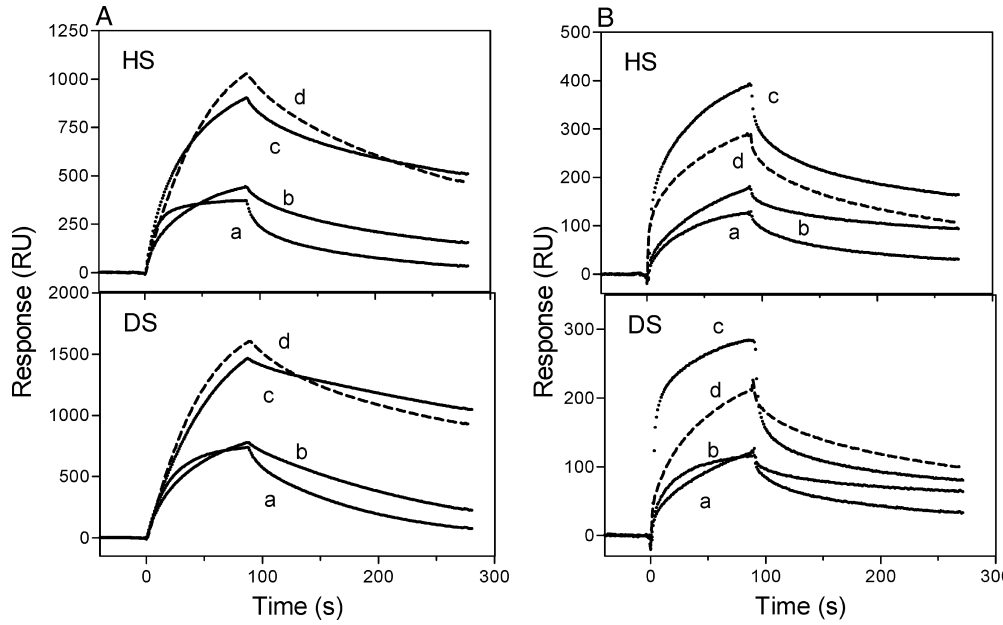

FIGURE 8: SPR sensorgrams of binding of apoE isoforms to HS and DS: apoE2 (a), apoE3 (b), apoE4 (c), and apoE4 E255A (d) in the lipid-free form (A) or DMPC discoidal complexes (B). The protein concentration was 30 μg/mL.

Table 2: Kinetic Parameters for Binding of DMPC Discoidal Complexes of ApoE Isoforms to HS

	k_{a1} ($\times 10^5$ M^{-1} s^{-1})	k_{d1} ($\times 10^{-2}$ s^{-1})	k_{a2} ($\times 10^{-2}$ s^{-1})	k_{d2} ($\times 10^{-3}$ s^{-1})	K_1 ($\times 10^5$ M^{-1})	K_2	K_d (μM)
apoE2−DMPC	0.4 ± 0.1	9.2 ± 2.7	1.5 ± 0.1	6.6 ± 2.0	4.4	2.3	0.68 ± 0.21
apoE3−DMPC	0.4 ± 0.1	13 ± 2	2.7 ± 0.1	3.4 ± 1.0	3.1	8.0	0.35 ± 0.15
apoE4−DMPC	1.1 ± 0.2	15 ± 3	1.6 ± 0.1	4.2 ± 1.0	7.5	4.0	0.27 ± 0.08

proposed a two-step mechanism for the apoE−heparin interaction, the first step involving a fast electrostatic interaction, followed by a slower hydrophobic interaction (*28*). In this study, we extended this approach to examine the role of the N- and C-terminal domains of apoE isoforms in their interactions with more physiological GAGs, HS and DS.

The current SPR data demonstrate that the binding of apoE to HS and DS involves a two-state binding process, similar to the situation with heparin. However, the large decreases in the association rate and the favorable free energy of binding in the first step observed for HS and DS compared to heparin (Figure 3) indicate that the contribution of the initial electrostatic interaction to the overall binding is smaller for HS and DS than for heparin (*26*). In addition, the mutation in lysine 146 which disrupts direct ionic interaction between basic residues on apoE and sulfate groups on the GAG chain (*26*) greatly reduced the favorable free energy for the first step of binding to HS and DS (Figure 4B). The reduction of this free energy from that of the WT (1.5 and 1.3 kcal/mol for HS and DS, respectively) was much smaller than that in heparin (2.7 kcal/mol) (Figure 6 in ref *28*). These results are consistent with the fact that heparin has an average of two to three sulfate groups per disaccharide, whereas HS and DS contain fewer than one sulfate per disaccharide (*31*). Comparison of the free energies of binding in the two processes (Figure 3) indicates that even in the less sulfated HS and DS, the electrostatic interaction still contributes greatly (>90%) to the overall free energy of binding of apoE to GAG. In fact, analysis of the dependence of K_d and R_{max} values on sodium chloride concentration for binding of the apoE3 22 kDa fragment to various GAGs showed that an increase in ionic strength greatly reduces both the affinity and saturated level of apoE binding to GAG (data not shown).

In contrast to the dominant role of the N-terminal site in apoE−GAG binding, the C-terminal site (basic residues around lysine 233) is not available for the interaction of full-length apoE with GAG (Figure 4) (*27, 28*). Rather, the C-terminal domain appears to contribute to the high-affinity binding of apoE to GAG through an oligomerization effect (*27*). Using C-terminally truncated mutants of apoE, we showed previously that the C-terminal helical residues, 261−299 or 272−299, modulate the tetramerization of apoE in solution (*37, 47*). As shown in Figure 5A, progressive truncation of the C-terminal helical segments which leads to the monomeric form greatly reduced the level of binding of apoE3 to HS. The fact that the C-terminal truncation mainly reduced the favorable free energy for the first binding step (Figure 5B) indicates that oligomerization through the C-terminal α-helical region has a major influence on the electrostatic interaction between apoE and GAG. This notion that multiple binding sites of apoE molecules increase the affinity of GAG binding is consistent with the previous study of peptides including heparin binding consensus sequences showing that multiple copies of the heparin binding site enhance the binding affinity through cooperativity effects (*51*). The findings that dimerization of the apoE3 22 kDa fragment via disulfide linkage markedly increased the level of binding to HS compared to the monomeric form (Figure 6) and restored the kinetic rate constants and equilibrium affinity in the first step to the level comparable to those of the full-length protein (Table 1) further support this idea. We found that the dimerization of the apoE3 22 kDa

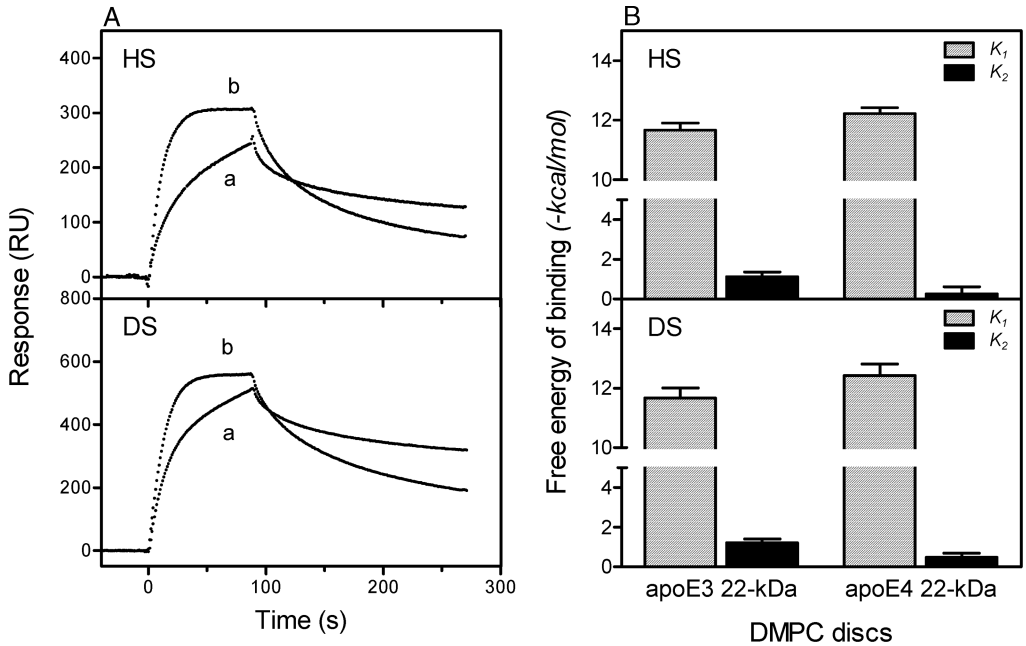

FIGURE 9: SPR sensorgrams (A) and free energies of binding (B) for the interaction of DMPC discoidal complexes of 22 kDa apoE3 and apoE4 with HS and DS. (A) DMPC discoidal complex of apoE3 22 kDa (a) and apoE4 22 kDa (b) fragments. The protein concentration was 3 μg/mL.

fragment destabilized the N-terminal helix bundle and exposed hydrophobic surface (data not shown). However, such a hydrophobic exposure contributes to the second step of GAG binding (*28*), whereas binding of the apoE3 22 kDa dimer to the GAG is associated with an increased contribution of the first step. This indicates that the dimerization enhances the electrostatic interaction in a manner similar to that in the case of the C-terminally truncated mutants. In this regard, the similar electrostatic interaction in GAG binding of full-length apoE3 in the lipid-free state and in a discoidal complex (Figure 7) may result from the fact that apoE is a tetramer in the lipid-free state and that there are approximately four apoE molecules bound to DMPC disks (*52*).

An important finding in this study is that apoE4 binds better to HS and DS than does apoE2 or apoE3 in both the lipid-free and lipidated forms (Figure 8). The fact that the E255A mutation did not significantly reduce the extent of binding of apoE4 indicates that the domain interaction in apoE4 is not mainly responsible for the greater binding of apoE4. Since apoE4 is less likely to self-associate than apoE3 in solution (*47*) and the number of apoE molecules on DMPC disks is similar among apoE isoforms (*52*), it is unlikely that the greater ability of binding of apoE4 to GAG is due to the cooperative effects of the heparin binding sites. Rather, it is likely that the greater electrostatic interaction through the N-terminal binding site of apoE4 leads to its greater binding ability to GAG (Figure 9). It is possible that the positively charged residues involved in the heparin binding in apoE4 have a different electrostatic potential compared to apoE3 (*49*), leading to the enhanced electrostatic interaction of apoE4 with GAG. Indeed, analysis of the dependence of affinity constants on sodium chloride concentration (*53, 54*) indicated that the number of purely ionic interactions involved in the HS binding of apoE4 is 3-fold larger than that for apoE3 (data not shown).

Such an improved ability of apoE4 to bind to GAG rather than other apoE isoforms gives important insight into the atherogenic or anti-atherogenic properties of apoE isoforms. The retention of lipoproteins in the arterial extracellular matrix is a critical step in atherogenesis in which lipoproteins with higher affinity for arterial proteoglycans are more atherogenic (*55, 56*). It was reported that apoE3 and apoE4 have different effects on HDL metabolism (*57*), and the interaction of apoE with CS and/or DS proteoglycans is responsible for the retention of HDL on the extracellular matrix of arterial smooth muscle cells (*14*). Since apoE4 appears to bind more strongly to cell-surface GAGs than apoE3 (*17*), apoE4-containing lipoproteins could be retained more than apoE3-containing lipoproteins by vascular proteoglycans, resulting in oxidative and other potential atherogenic modifications like serum amyloid A-containing HDL (*58*). Thus, besides being a risk factor for Alzheimer's disease, apoE4 is associated with an increased risk for coronary heart disease (*7*).

In summary, we have characterized the role of the N- and C-terminal domains in the interaction of apoE isoforms with GAG using an SPR approach. The N-terminal binding site dominantly contributes to the electrostatic interaction of apoE with GAG, whereas the C-terminal domain facilitates this electrostatic interaction through cooperative effects. The enhanced electrostatic interaction with apoE4 compared to apoE3 appears to underlie the stronger binding of apoE4 to GAG, probably explaining the different retentions of apoE isoform-containing lipoproteins in the arterial wall.

REFERENCES

1. Salmivirta, M., Lidholt, K., and Lindahl, U. (1996) Heparan sulfate: A piece of information. *FASEB J. 10*, 1270–1279.
2. Mahley, R. W., and Huang, Y. (2007) Atherogenic remnant lipoproteins: Role for proteoglycans in trapping, transferring, and internalizing. *J. Clin. Invest. 117*, 94–98.

3. Williams, K. J., Liu, M. L., Zhu, Y., Xu, X., Davidson, W. R., McCue, P., and Sharma, K. (2005) Loss of heparan N-sulfotransferase in diabetic liver: Role of angiotensin II. *Diabetes 54*, 1116–1122.
4. Ebara, T., Conde, K., Kako, Y., Liu, Y., Xu, Y., Ramakrishnan, R., Goldberg, I. J., and Shachter, N. S. (2000) Delayed catabolism of apoB-48 lipoproteins due to decreased heparan sulfate proteoglycan production in diabetic mice. *J. Clin. Invest. 105*, 1807–1818.
5. Mahley, R. W. (1988) Apolipoprotein E: Cholesterol transport protein with expanding role in cell biology. *Science 240*, 622–630.
6. Cooper, A. D. (1997) Hepatic uptake of chylomicron remnants. *J. Lipid Res. 38*, 2173–2192.
7. Mahley, R. W., and Rall, S. C., Jr. (2000) Apolipoprotein E: Far more than a lipid transport protein. *Annu. Rev. Genomics Hum. Genet. 1*, 507–537.
8. Mahley, R. W., and Ji, Z. S. (1999) Remnant lipoprotein metabolism: Key pathways involving cell-surface heparan sulfate proteoglycans and apolipoprotein E. *J. Lipid Res. 40*, 1–16.
9. Swertfeger, D. K., and Hui, D. Y. (2001) Apolipoprotein E: Receptor versus heparan sulfate proteoglycan binding in its regulation of smooth muscle cell migration and proliferation. *J. Biol. Chem. 276*, 25043–25048.
10. Holtzman, D. M., Pitas, R. E., Kilbridge, J., Nathan, B., Mahley, R. W., Bu, G., and Schwartz, A. L. (1995) Low density lipoprotein receptor-related protein mediates apolipoprotein E-dependent neurite outgrowth in a central nervous system-derived neuronal cell line. *Proc. Natl. Acad. Sci. U.S.A. 92*, 9480–9484.
11. Ji, Z. S., Pitas, R. E., and Mahley, R. W. (1998) Differential cellular accumulation/retention of apolipoprotein E mediated by cell surface heparan sulfate proteoglycans. Apolipoproteins E3 and E2 greater than E4. *J. Biol. Chem. 273*, 13452–13460.
12. Bazin, H. G., Marques, M. A., Owens, A. P., III, Linhardt, R. J., and Crutcher, K. A. (2002) Inhibition of apolipoprotein E-related neurotoxicity by glycosaminoglycans and their oligosaccharides. *Biochemistry 41*, 8203–8211.
13. Burgess, J. W., Liang, P., Vaidyanath, C., and Marcel, Y. L. (1999) ApoE of the HepG2 cell surface includes a major pool associated with chondroitin sulfate proteoglycans. *Biochemistry 38*, 524–531.
14. Olin-Lewis, K., Benton, J. L., Rutledge, J. C., Baskin, D. G., Wight, T. N., and Chait, A. (2002) Apolipoprotein E mediates the retention of high-density lipoproteins by mouse carotid arteries and cultured arterial smooth muscle cell extracellular matrices. *Circ. Res. 90*, 1333–1339.
15. Rapp, A., and Huttinger, M. (2005) Role of chondroitin sulphate in the uptake of β-VLDL by brain cells. *Eur. J. Neurosci. 22*, 1400–1408.
16. Lin, C.-Y., Huang, Z. H., and Mazzone, T. (2001) Interaction with proteoglycans enhances the sterol efflux produced by endogenous expression of macrophage apoE. *J. Lipid Res. 42*, 1125–1133.
17. Hara, M., Matsushima, T., Satoh, H., Iso-o, N., Noto, H., Togo, M., Kimura, S., Hashimoto, Y., and Tsukamoto, K. (2003) Isoform-dependent cholesterol efflux from macrophages by apolipoprotein E is modulated by cell surface proteoglycans. *Arterioscler. Thromb. Vasc. Biol. 23*, 269–274.
18. Weisgraber, K. H. (1994) Apolipoprotein E: Structure-function relationships. *Adv. Protein Chem. 45*, 249–302.
19. Hatters, D. M., Peters-Libeu, C. A., and Weisgraber, K. H. (2006) Apolipoprotein E structure: Insights into function. *Trends Biochem. Sci. 31*, 445–454.
20. Wilson, C., Wardell, M. R., Weisgraber, K. H., Mahley, R. W., and Agard, D. A. (1991) Three-dimensional structure of the LDL receptor-binding domain of human apolipoprotein E. *Science 252*, 1817–1822.
21. Westerlund, J. A., and Weisgraber, K. H. (1993) Discrete carboxyl-terminal segments of apolipoprotein E mediate lipoprotein association and protein oligomerization. *J. Biol. Chem. 268*, 15745–15750.
22. Saito, H., Dhanasekaran, P., Baldwin, F., Weisgraber, K. H., Lund-Katz, S., and Phillips, M. C. (2001) Lipid binding-induced conformational change in human apolipoprotein E. Evidence for two lipid-bound states on spherical particles. *J. Biol. Chem. 276*, 40949–40954.
23. Cardin, A. D., Hirose, N., Blankenship, D. T., Jackson, R. L., Harmony, J. A., Sparrow, D. A., and Sparrow, J. T. (1986) Binding of a high reactive heparin to human apolipoprotein E: Identification of two heparin-binding domains. *Biochem. Biophys. Res. Commun. 134*, 783–789.
24. Weisgraber, K. H., Rall, S. C., Mahley, R. W., Milne, R. W., Marcel, Y. L., and Sparrow, J. T. (1986) Human apolipoprotein E. Determination of the heparin binding sites of apolipoprotein E3. *J. Biol. Chem. 261*, 2068–2076.
25. Dong, J., Peters-Libeu, C. A., Weisgraber, K. H., Segelke, B. W., Rupp, B., Capila, I., Hernaiz, M. J., LeBrun, L. A., and Linhardt, R. J. (2001) Interaction of the N-terminal domain of apolipoprotein E4 with heparin. *Biochemistry 40*, 2826–2834.
26. Libeu, C. P., Lund-Katz, S., Phillips, M. C., Wehrli, S., Hernaiz, M. J., Capila, I., Linhardt, R. J., Raffai, R. L., Newhouse, Y. M., Zhou, F., and Weisgraber, K. H. (2001) New insights into heparan sulfate proteoglycan-binding activity of apolipoprotein E. *J. Biol. Chem. 276*, 39138–39144.
27. Saito, H., Dhanasekaran, P., Nguyen, D., Baldwin, F., Weisgraber, K. H., Wehrli, S., Phillips, M. C., and Lund-Katz, S. (2003) Characterization of the heparin binding sites in human apolipoprotein E. *J. Biol. Chem. 278*, 14782–14787.
28. Futamura, M., Dhanasekaran, P., Handa, T., Phillips, M. C., Lund-Katz, S., and Saito, H. (2005) Two-step mechanism of binding of apolipoprotein E to heparin: Implications for the kinetics of apolipoprotein E-heparan sulfate proteoglycan complex formation on cell surfaces. *J. Biol. Chem. 280*, 5414–5422.
29. Klezovitch, O., Formato, M., Cherchi, G. M., Weisgraber, K. H., and Scanu, A. M. (2000) Structural determinants in the C-terminal domain of apolipoprotein E mediating binding to the protein core of human aortic biglycan. *J. Biol. Chem. 275*, 18913–18918.
30. Klezovitch, O., and Scanu, A. M. (2001) Domains of apolipoprotein E involved in the binding to the protein core of biglycan of the vascular extracellular matrix: Potential relationship between retention and anti-atherogenic properties of this apolipoprotein. *Trends Cardiovasc. Med. 11*, 263–268.
31. Hileman, R. E., Fromm, J. R., Weiler, J. M., and Linhardt, R. J. (1998) Glycosaminoglycan-protein interactions: Definition of consensus sites in glycosaminoglycan binding proteins. *BioEssays 20*, 156–167.
32. Olsson, U., Ostergren-Lunden, G., and Moses, J. (2001) Glycosaminoglycan-lipoprotein interaction. *Glycoconjugate J. 18*, 789–797.
33. Capila, I., and Linhardt, R. J. (2002) Heparin-protein interactions. *Angew. Chem., Int. Ed. 41*, 391–412.
34. Shuvaev, V. V., Laffont, I., and Siest, G. (1999) Kinetics of apolipoprotein E isoforms binding to the major glycosaminoglycans of the extracellular matrix. *FEBS Lett. 459*, 353–357.
35. Lundquist, P., Martensson, J., Sorbo, B., and Ohman, S. (1980) Turbidimetry of inorganic sulfate, ester sulfate, and total sulfur in urine. *Clin. Chem. 26*, 1178–1181.
36. Saito, H., Dhanasekaran, P., Baldwin, F., Weisgraber, K. H., Phillips, M. C., and Lund-Katz, S. (2003) Effects of polymorphism on the lipid interaction of human apolipoprotein E. *J. Biol. Chem. 278*, 40723–40729.
37. Tanaka, M., Vedhachalam, C., Sakamoto, T., Dhanasekaran, P., Phillips, M. C., Lund-Katz, S., and Saito, H. (2006) Effect of carboxyl-terminal truncation on structure and lipid interaction of human apolipoprotein E4. *Biochemistry 45*, 4240–4247.
38. Lund-Katz, S., Zaiou, M., Wehrli, S., Dhanasekaran, P., Baldwin, F., Weisgraber, K. H., and Phillips, M. C. (2000) Effects of lipid interaction on the lysine microenvironments in apolipoprotein E. *J. Biol. Chem. 275*, 34459–34464.
39. Raut, S., and Gaffney, P. J. (1996) Interaction of heparin with fibrinogen using surface plasmon resonance technology: Investigation of heparin binding site on fibrinogen. *Thromb. Res. 81*, 503–509.
40. Lin, Y., Pixley, R. A., and Colman, R. W. (2000) Kinetic analysis of the role of zinc in the interaction of domain 5 of high-molecular weight kininogen (HK) with heparin. *Biochemistry 39*, 5104–5110.
41. Myszka, D. G. (1997) Kinetic analysis of macromolecular interactions using surface plasmon resonance biosensors. *Curr. Opin. Biotechnol. 8*, 50–57.
42. Karlsson, R., and Falt, A. (1997) Experimental design for kinetic analysis of protein-protein interactions with surface plasmon resonance biosensors. *J. Immunol. Methods 200*, 121–133.
43. Lipschultz, C. A., Li, Y., and Smith-Gill, S. (2000) Experimental design for analysis of complex kinetics using surface plasmon resonance. *Methods 20*, 310–318.
44. Morrisett, J. D., David, J. S., Pownall, H. J., and Gotto, A. M., Jr. (1973) Interaction of an apolipoprotein (apoLP-alanine) with phosphatidylcholine. *Biochemistry 12*, 1290–1299.
45. Aggerbeck, L. P., Wetterau, J. R., Weisgraber, K. H., Wu, C. S., and Lindgren, F. T. (1988) Human apolipoprotein E3 in aqueous

solution. II. Properties of the amino- and carboxyl-terminal domains. *J. Biol. Chem. 263*, 6249–6258.
46. Zhang, Y., Vasudevan, S., Sojitrawala, R., Zhao, W., Cui, C., Xu, C., Fan, D., Newhouse, Y., Balestra, R., Jerome, W. G., Weisgraber, K., Li, Q., and Wang, J. (2007) A monomeric, biologically active, full-length human apolipoprotein E. *Biochemistry 46*, 10722–10732.
47. Sakamoto, T., Tanaka, M., Vedhachalam, C., Nickel, M., Nguyen, D., Dhanasekaran, P., Phillips, M. C., Lund-Katz, S., and Saito, H. (2008) Contributions of the carboxyl-terminal helical segment to the self-association and lipoprotein preferences of human apolipoprotein E3 and E4 isoforms. *Biochemistry 47*, 2968–2977.
48. Dong, L. M., and Weisgraber, K. H. (1996) Human apolipoprotein E4 domain interaction. Arginine 61 and glutamic acid 255 interact to direct the preference for very low density lipoproteins. *J. Biol. Chem. 271*, 19053–19057.
49. Lund-Katz, S., Wehrli, S., Zaiou, M., Newhouse, Y., Weisgraber, K. H., and Phillips, M. C. (2001) Effects of polymorphism on the microenvironment of the LDL receptor-binding region of human apoE. *J. Lipid Res. 42*, 894–901.
50. MacArthur, J. M., Bishop, J. R., Stanford, K. I., Wang, L., Bensadoun, A., Witztum, J. L., and Esko, J. D. (2007) Liver heparan sulfate proteoglycans mediate clearance of triglyceride-rich lipoproteins independently of LDL receptor family members. *J. Clin. Invest. 117*, 153–164.
51. Verrecchio, A., Germann, M. W., Schick, B. P., Kung, B., Twardowski, T., and San Antonio, J. D. (2000) Design of peptides with high affinities for heparin and endothelial cell proteoglycans. *J. Biol. Chem. 275*, 7701–7707.
52. Schneeweis, L. A., Koppaka, V., Lund-Katz, S., Phillips, M. C., and Axelsen, P. H. (2005) Structural analysis of lipoprotein E particles. *Biochemistry 44*, 12525–12534.
53. Goncalves, E., Kitas, E., and Seelig, J. (2006) Structural and thermodynamic aspects of the interaction between heparan sulfate and analogues of melittin. *Biochemistry 45*, 3086–3094.
54. Klocek, G., and Seelig, J. (2008) Melittin interaction with sulfated cell surface sugars. *Biochemistry 47*, 2841–2849.
55. Williams, K. J., and Tabas, I. (1995) The response-to-retention hypothesis of early atherogenesis. *Arterioscler. Thromb. Vasc. Biol. 15*, 551–561.
56. Gustafsson, M., and Boren, J. (2004) Mechanism of lipoprotein retention by the extracellular matrix. *Curr. Opin. Lipidol. 15*, 505–514.
57. Hopkins, P. C., Huang, Y., McGuire, J. G., and Pitas, R. E. (2002) Evidence for differential effects of apoE3 and apoE4 on HDL metabolism. *J. Lipid Res. 43*, 1881–1889.
58. Lewis, K. E., Kirk, E. A., McDonald, T. O., Wang, S., Wight, T. N., O'Brien, K. D., and Chait, A. (2004) Increase in serum amyloid a evoked by dietary cholesterol is associated with increased atherosclerosis in mice. *Circulation 110*, 540–545.

BI8003999